

Accepted Manuscript

Title: Synergistic effect between CaCl_2 and $\gamma\text{-Al}_2\text{O}_3$ for furfural production by dehydration of hemicellulosic carbohydrates

Authors: I. Fúnez-Núñez, C. García-Sancho, J.A. Cecilia, R. Moreno-Tost, E. Pérez-Inestrosa, L. Serrano-Cantador, P. Maireles-Torres



PII: S0926-860X(19)30343-6
DOI: <https://doi.org/10.1016/j.apcata.2019.117188>
Article Number: 117188

Reference: APCATA 117188

To appear in: *Applied Catalysis A: General*

Received date: 6 May 2019
Revised date: 31 July 2019
Accepted date: 1 August 2019

Please cite this article as: Fúnez-Núñez I, García-Sancho C, Cecilia JA, Moreno-Tost R, Pérez-Inestrosa E, Serrano-Cantador L, Maireles-Torres P, Synergistic effect between CaCl_2 and $\gamma\text{-Al}_2\text{O}_3$ for furfural production by dehydration of hemicellulosic carbohydrates, *Applied Catalysis A, General* (2019), <https://doi.org/10.1016/j.apcata.2019.117188>

This is a PDF file of an unedited manuscript that has been accepted for publication. As a service to our customers we are providing this early version of the manuscript. The manuscript will undergo copyediting, typesetting, and review of the resulting proof before it is published in its final form. Please note that during the production process errors may be discovered which could affect the content, and all legal disclaimers that apply to the journal pertain.

**Synergistic effect between CaCl₂ and γ -Al₂O₃ for furfural production by
dehydration of hemicellulosic carbohydrates**

I. Fúnez-Núñez^a, C. García-Sancho^{a*}, J.A. Cecilia^a, R. Moreno-Tost^a, E. Pérez-
Inestrosa^{b,c}, L. Serrano-Cantador^d, P. Maireles-Torres^a

^a *Universidad de Málaga, Departamento de Química Inorgánica, Cristalografía y
Mineralogía (Unidad Asociada al ICP-CSIC), Facultad de Ciencias, Campus de
Teatinos, 29071 Málaga, Spain*

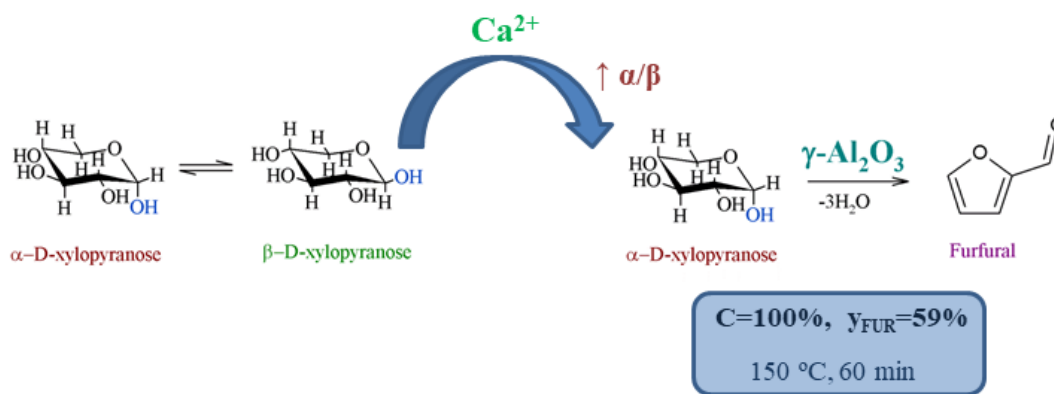
^b *Andalusian Center for Nanomedicine and Biotechnology - BIONAND, Málaga,
Spain*

^c *Department of Organic Chemistry, University of Málaga, IBIMA, Málaga, Spain*

^d *Universidad de Córdoba. Departamento de Química Inorgánica e Ingeniería Química.
Campus Universitario de Rabanales, Edificio Marie Curie (C3). Ctra. (a) de Madrid,
km 396, 14071-Córdoba.*

**Corresponding author: cristinags@uma.es*

Graphical abstract



Highlights

- CaCl_2 increases the α -xylopyranose/ β -xylopyranose ratio favoring the xylose dehydration with respect to other salts and $\gamma\text{-Al}_2\text{O}_3$ promotes the furfural production due to their Lewis acid sites.
- The synergistic effect between CaCl_2 and $\gamma\text{-Al}_2\text{O}_3$ gives full conversion and furfural yield of 55% after 50 min at 150°C and $\gamma\text{-Al}_2\text{O}_3$ can be reused at least for 10 catalytic runs without regeneration.
- CaCl_2 and $\gamma\text{-Al}_2\text{O}_3$ provided a furfural yield of 83% by liquors obtained from olive stones demonstrating their applicability for furfural production from lignocellulosic biomass.

Abstract

γ -Al₂O₃ has successfully been used as solid acid catalyst for xylose dehydration in a water:toluene biphasic system. The addition of alkaline earth metal chlorides improved the partition coefficient, thus facilitating the extraction of furfural from the aqueous phase. In this sense, the best catalytic performance was attained by using CaCl₂ and γ -Al₂O₃ with almost full xylose conversion and a furfural yield of 55% after 50 min, at 150°C. A ¹H NMR study has demonstrated that CaCl₂ shifts the α -xylopyranose/ β -xylopyranose anomeric equilibrium toward the α -form, more favorable for initiating the dehydration process, and γ -Al₂O₃ promotes the furfural production. γ -Al₂O₃ can be reused during ten catalytic cycles without any pretreatment. Finally, the synergistic effect between CaCl₂ and γ -Al₂O₃ could also be inferred from the increase in furfural yield, until a value of 83% after 50 min at 175°C, by using a hemicellulosic liquor obtained from olive stones.

Keywords: *lignocellulose; alumina; calcium chloride; furfural; xylose; olive stones*

1. Introduction

The development of environmentally and economically viable synthetic routes and technologies in order to obtain chemicals and fuels by using non-fossil carbon sources has been reenergized in recent years in order to replace fossil fuels [1]. In this context, biomass is a very promising sustainable feedstock due to its availability and it can be employed as renewable carbon source [2-4]. In particular, lignocellulosic biomass is the most abundant ($2 \cdot 10^{11}$ metric tons per year) and it is mainly composed by three compounds (lignin, cellulose and hemicellulose), being necessary its full fractioning and valorization for the profitability of its use as a raw material [5]. However, lignocellulose will be a sustainable resource for production of biofuels and

chemicals as long as the biomass does not interfere with the food chain. In particular, hemicellulose is made up of amorphous heteropolysaccharides, containing five and six carbon units, which can be substituted with phenolic, uronic or acetyl groups [6]. The pentoses, xylose and arabinose, are the main and more abundant monomers, although hexoses such as glucose, mannose and galactose are found in minor proportions. From biomass waste, hemicellulosic carbohydrates can be recovered by different physicochemical processes for the production of chemicals, such as xylitol, lactic acid or furfural [7].

The acid hydrolysis of hemicellulose leads to pentoses, mainly xylose, whose dehydration gives rise to furfural. Furfural is a key building block produced in lignocellulose-based biorefineries, which could further be transformed to fuels and useful chemicals, being widely used in oil refining, plastics, pharmaceutical and agrochemical industries [8]. Considering that xylose is the most abundant carbohydrate present in hemicellulose, great efforts have been carried out to study its dehydration into furfural. One of the main problems in the production of furfural is related to the existence of other unwanted side reactions, which may occur at the same time as dehydration, decreasing the furfural yield. Thus, fragmentation reactions of furfural can take place, leading to the formation of formaldehyde, formic acid, acetaldehyde, dihydroxyacetone, glyceraldehyde, glycolaldehyde, lactic acid, acetol and pyruvaldehyde [9, 10]. Likewise, condensation reactions between furfural and the reaction intermediates from xylose have usually been observed, although in the absence of xylose these reactions do not take place [11]. Besides, furfural reactions with itself can give rise to resinification products [10]. On the other hand, it is well known that the dehydration of xylose requires the presence of acid sites to yield furfural. Weingarten *et*

al. reported that both Brønsted and Lewis acid sites catalyze xylose dehydration into furfural, being the latter more active but less selective since condensation reactions take place preferentially on Lewis acid sites [12].

Nevertheless, both solvent and catalyst are considered as two key factors to attain high furfural yields from xylose dehydration. The use of biphasic systems for furfural production has gained attention, because this approach can allow achieving higher furfural yields than those systems employing only water [13-15]. A biphasic medium, formed by the addition of immiscible organic solvents, such as toluene [16], methyl isobutyl ketone [17] and alkylphenols [15] to a diluted acid solution, or the addition of miscible organic solvents such as γ -valerolactone (GVL) [18] or tetrahydrofuran (THF) [19], to a saturated salt solution, allows to extract the target product, i.e. furfural, from the aqueous phase, preventing its further degradation and condensation.

Likewise, a large variety of solid acid catalysts as alternative to conventional mineral acids has been studied for the dehydration of xylose to furfural: zeolites [20], heteropolyacids [21], ion exchange resins [22] and metal oxides and phosphates [23, 24], either pure or supported to improve their textural properties. Several reviews have been published dealing with the dehydration of xylose to furfural [10, 25-27]. Thus, aluminum oxides have been traditionally employed as supports and catalysts due to their abundance, price and availability. The catalytic behavior of alumina, as such or in mixed oxides, has been evaluated for dehydration of different carbohydrates, such as glucose, fructose or xylose [28-33]. In particular, in a previous study, it was demonstrated that the use of γ -Al₂O₃ as support for Nb₂O₅ based catalysts enhanced

xylose conversion in its dehydration into furfural, although it promoted side reactions and considerably decreased the furfural selectivity [28].

In order to prevent these side reactions, the use of inorganic salts has been proposed in the literature. Marcotullio *et al.* [34, 35] found that halide anions promoted the formation of 1,2-enediol as acyclic intermediate for xylose dehydration, which was subsequently dehydrated to furfural. Enslow *et al.* [36] demonstrated that xylose is quickly transformed in the presence of aqueous solutions of inorganic salts, in comparison with pure water, and its rate depended on the nature of both cation and anion. However, other conclusions about the effect of inorganic salts on the dehydration of sugars have been reached by using other carbohydrates. Thus, Rasrendra *et al.* [37] determined, from the study of different metal halide and sulfate salts, that the influence of anion was less relevant than the effect of cations. Román-Leshkov *et al.* [38] employed inorganic salts in a biphasic system in order to obtain HMF from fructose; they concluded that the catalytic improvement attained in the presence of salts could be attributed to the interaction of both cationic and anionic species. On the other hand, it has been reported that divalent cations interact more strongly with saccharides than the monovalent ones [39, 40]. Thus, Combs *et al.* [41] observed that alkaline earth metal cations can interact with glucose, forming bidentate complexes, which accelerated its transformation. Later, our research group studied the beneficial effects of CaCl_2 on glucose dehydration to HMF in the presence of Al_2O_3 as catalyst, in such a way that the addition of CaCl_2 notably enhanced the HMF production, even at very short reaction times, since the presence of Ca^{2+} promoted the α -D-glucopyranose formation [42]. Therefore, it would be possible that alkaline earth cations exert a similar effect on the dehydration of xylose.

In this work, the dehydration of xylose to furfural has been evaluated by using a mesoporous γ -Al₂O₃ with acid character, in a biphasic water-toluene solvent system to minimize side reactions involving furfural. The addition of inorganic salts, such as CaCl₂ and MgCl₂, to the reaction medium has been carried out in order to maximize the furfural yield. Likewise, the role of these alkaline earth metal salts into the mechanistic pathways has been elucidated for the first time by ¹H NMR. Different experimental parameters, such as the reaction time, the temperature, the amount of catalyst and its possible reuse and the influence of the amount of inorganic salts to the reaction medium, have also been evaluated. In addition, the catalytic performance of γ -Al₂O₃ and/or CaCl₂ has been studied with liquors obtained from the treatment of olive stones, as lignocellulosic biomass.

2. Experimental

2.1. Reagents

The following chemicals have been used for the catalytic tests: alumina (Alfa-Aesar, Brockmann Grade I, 58 Å), xylose (Sigma-Aldrich, >99%), deionized water and toluene (VWR, 98%) as solvents and CaCl₂·2H₂O (VWR, 97%) and MgCl₂·6H₂O (VWR, 99%) as alkaline earth salts.

2.2. Characterization of catalysts

The textural parameters were determined from the N₂ adsorption-desorption isotherms at -196 °C by using a gas adsorption analyser (ASAP, Micromeritics). The sample was previously degassed at 200 °C and 10⁻⁴ mbar for 10 h. The Brunauer-Emmet-Teller (BET) equation was utilized to determine surface area taking a N₂ cross

section of 16.2 \AA^2 and the BJH method was employed to calculate the pore size distribution.

The total surface acidity of catalyst was evaluated by the temperature-programmed desorption of ammonia (NH_3 -TPD). Firstly, the cleaning of catalyst (80 mg) was carried out under a helium flow at $550 \text{ }^\circ\text{C}$. Later, the adsorption of ammonia took place at $100 \text{ }^\circ\text{C}$ and the NH_3 -TPD was realized by increasing the temperature from 100 to $550 \text{ }^\circ\text{C}$ ($10 \text{ }^\circ\text{C min}^{-1}$) and maintaining at $550 \text{ }^\circ\text{C}$ for 15 min under a helium flow of 40 mL min^{-1} . The evolved ammonia was determined by using a Thermal Conductivity Detector.

FTIR spectra of adsorbed pyridine were recorded on a Shimadzu Fourier Transform Infrared Instrument (FTIR8300). Self-supported wafer of the sample with a weight/surface ratio of about 15 mg cm^{-2} was placed in a vacuum cell greaseless stopcocks and CaF_2 windows. The sample was evacuated at $300 \text{ }^\circ\text{C}$ and 10^{-2} Pa overnight, exposed to pyridine vapors at room temperature (vapor pressure of 200 mbar) for 10 min and then outgassed at room temperature, $100 \text{ }^\circ\text{C}$ and $200 \text{ }^\circ\text{C}$.

Thermogravimetric analyses (TGA) were performed under air flow of 50 mL min^{-1} by a TGA/DSC 1 model (Mettler-Toledo) from $30 \text{ }^\circ\text{C}$ until $900 \text{ }^\circ\text{C}$ with a heating ramp of $10 \text{ }^\circ\text{C min}^{-1}$. The carbon content of the spent catalyst was determined with a LECO CHNS 932 analyzer.

The leaching of Al species was carried out on an ICP-MS Nexión 300D by using a software NexION (Perkin Elmer) to calculate the concentration.

2.3. Catalytic tests

The furfural production from the catalytic dehydration of xylose was carried out under batch conditions with magnetic stirring, by using a glass pressure tube with thread bushing (Ace, 15 mL). In a typical experiment, 0.05 g of catalyst, 0.15 g of xylose, 1.5 mL of deionized water and 3.5 mL of toluene as solvent and co-solvent respectively were poured into the reactor. The reaction temperature was controlled with a thermocouple in an oil bath. In order to avoid the secondary reactions, reactors were always purged with N₂ prior the experiments. The reaction was quenched by submerging the reactor in a cool water bath. Both organic and aqueous phases were separated, filtered and the products were analyzed by high performance liquid chromatography (HPLC), being xylose and furfural the only detected products. A JASCO instrument equipped with two detectors, multiwavelength detector (MD-2015) and refraction index (RI-2031), a quaternary gradient pump (PU-2089), autosampler (AS-2055), column oven (co-2065) and two columns, Phenomenex Luna C18 reversed-phase column (250 mm × 4.6 mm, 5 μm) and Phenomenex Rezex ROA-Organic Acid H⁺ (8%) (300 mm × 7.8 mm, 5 μm), was employed. Xylose was monitored using a refractive index detector in the aqueous phase, while furfural production was monitored using multiwavelength detector in both phases, water and toluene (278 and 285 nm respectively). The mobile phases consisted in pure methanol (flow rate 0.5 mL·min⁻¹) for Luna C18 and 0.005M H₂SO₄ aqueous solution (flow rate 0.35 mL·min⁻¹) for Rezex ROA-Organic Acid H⁺, being the columns at room temperature and 40 °C, respectively.

Moreover, the catalyst was reused for several catalytic runs, at 150 °C and 50 minutes, in the presence of 0.65 g·CaCl₂·g_{·aq.sol.}⁻¹. For this, the catalyst was kept inside the reactor after each cycle, and, without any pre-treatment, a new reaction mixture (xylose, CaCl₂, water and toluene) was added to carry out the reaction under identical

experimental conditions. On the other hand, the catalyst was washed by vacuum filtration, after the first reaction cycle, with a controlled amount of 10 mL of both water and toluene for its characterization, and these solvents were analyzed after washing by HPLC for analyzing both phases.

Finally, liquors from lignocellulosic biomass were prepared from olive stones by using a solid:water mass ratio of 1:20, at 180 °C for 30 min, in a temperature-controlled stainless-steel reactor (2 L) under batch conditions. These extraction conditions were based on results previously reported by Amendola et al. [43]. For the catalytic study, 1.5 mL of this liquor was taken as aqueous phase, and the same experimental conditions previously described for the tests with xylose were employed.

3. Results and discussion

It is well known that both the textural properties and the acidity of catalysts are key parameters to maximize the furfural yield [44]. Regarding the textural properties of γ -Al₂O₃ obtained from nitrogen adsorption-desorption data, a Type IV isotherm which trends to a Type II isotherm according to the IUPAC classification was found which confirmed its mesoporous character (Fig. 1A). In addition, the catalyst shows a high BET surface area (158 m²·g⁻¹) and large average pore diameter (4.7 nm) (Table 1) included in the range of mesopores, giving rise to a narrow pore size distribution (Fig. 1B).

On other hand the existence of acid sites with different strength, and a high total acidity (478 μ moles NH₃·g_{cat}⁻¹) were demonstrated by the NH₃-desorption profile (Fig. 2 and Table 1). A maximum desorption at 180°C demonstrates the presence of weak acid sites, whereas the desorption at high temperatures is associated to strong acid sites [45].

The high values of BET surface area and total acidity make this catalyst displays higher amount of available acid sites since it presents an acid density equal to $3.02 \mu\text{moles NH}_3 \cdot \text{m}^{-2}$.

Likewise, it is relevant to know the nature of these acid centers which have been elucidated by adsorption of pyridine coupled to FTIR spectroscopy (Fig. 3). Thus, the absorption bands appearing at 1613 and 1449 cm^{-1} correspond to the 8a and 19b vibration modes of pyridine coordinated to strong Lewis acid sites (s-LAS), respectively [46]. In addition, it can be observed that although the outgassing temperature increases, the characteristic signal of pyridine adsorbed on these Lewis acid centers remains, although less intense, which corroborates the strength of Lewis acid sites. The band located at 1578 cm^{-1} is attributed to pyridine coordinated on weak Lewis acid sites (w-LAS), as was previously pointed out by Gallo *et al.* [46]. The intensity of this latter band decreases with the outgassing temperature, confirming the weakness of these acid sites. The existence of strong and weak Lewis acid sites could be inferred from its NH_3 -TPD curve. The absence of peaks around 1550 cm^{-1} demonstrates that $\gamma\text{-Al}_2\text{O}_3$ does not possess Brønsted acid sites (BAS). Another band is also detected at 1491 cm^{-1} which is usually associated to the 19a vibration mode of pyridine associated to both Brønsted and Lewis acid sites [47], being in this case only due to LAS. Finally, a band centered at 1594 cm^{-1} is also detected when pyridine is evacuated at room temperature, which can be assigned to the 8a vibration mode of pyridine bonded by hydrogen bond to the hydroxyl groups of the catalyst surface [48]. However, this band almost disappears after thermal treatment at $100 \text{ }^\circ\text{C}$, evidencing the weak interaction of pyridine with surface hydroxyl groups.

The γ - Al_2O_3 catalyst was employed for dehydration of xylose into furfural. It has previously been demonstrated that Lewis acid sites are more active than Brønsted ones, but less selective, since Lewis acid sites can promote condensation reactions [12]. γ - Al_2O_3 possesses weak and strong Lewis acid sites, as inferred from NH_3 -TPD and pyridine adsorption coupled to FTIR spectroscopy. However, Lewis acid sites can promote secondary reactions, leading to a low furfural selectivity, in spite of a high catalytic activity in xylose dehydration [28]. Therefore, it is necessary to optimize experimental conditions in order to maximize the furfural yield. In this sense, the use of biphasic systems can facilitate the continuous extraction of furfural formed from the aqueous phase, thus reducing its residence time in the aqueous phase for preventing the reaction with xylose and reaction intermediates [14, 49, 50]. In this work, a biphasic water-toluene system has been employed to obtain furfural from xylose dehydration by using γ - Al_2O_3 as solid acid catalyst and compared with the non-catalyzed process at 175 °C and 50 min of reaction (Fig. 4A). It was observed that the addition of γ - Al_2O_3 to the reaction medium considerably enhances the conversion of xylose and the furfural yield (86% and 26%, respectively) with respect to non-catalyzed process (15% and 14%, respectively). However, furfural yield is not very high in spite of the high catalytic activity of γ - Al_2O_3 .

Considering that the Lewis acid sites of γ - Al_2O_3 could favor the side reactions that decrease the furfural selectivity, the optimization of other reaction parameters has been performed to inhibit these side reactions, such as the addition of inorganic salts. In recent years, different authors have demonstrated the positive effect of adding inorganic salts for the production of HMF and furfural [35-42, 51, 52]. In this context, HMF yield obtained from dehydration of glucose was successfully improved by using calcium

chloride, achieving a maximum yield in presence of $0.65 \text{ g}_{\text{CaCl}_2} \cdot \text{g}_{\text{aq.sol.}}^{-1}$, since the Ca^{2+} ions interacted with glucose molecules favoring the α -D-glucopyranose formation, the most favorable anomer for enhancing HMF yield [42]. Thus, in the present work, a similar concentration of CaCl_2 has been utilized for dehydration of xylose to favor furfural production, as well as another alkaline earth metal salt, MgCl_2 , under equimolar concentration ($0.39 \text{ g} \cdot \text{g}_{\text{aq.sol.}}^{-1}$), in order to evaluate the effect of the cation nature (Fig. 4A). Although both salts improved the catalytic performance, the addition of CaCl_2 demonstrated to be more beneficial than MgCl_2 , attaining a xylose conversion of 96% and a furfural yield of 71%. In addition, it can be observed that the furfural production is higher using only CaCl_2 (71%) in the reaction medium than together with alumina (55%). It should be noted that the use of toluene as co-solvent provided higher values of furfural yield with respect to those attained for catalytic test by using only water as solvent (Fig. 4A). In order to get insights into the effect of these salts, the partition coefficients, R , defined as the furfural concentration in the organic phase with respect to the furfural concentration in the aqueous phase, have been determined. Thus, a positive effect has been detected increasing the R values in the presence of alumina and/or alkaline earth salts with respect to the catalytic test carried out in the absence of salt ($R = 0.52$) (Fig. 4B). Moreover, a direct relationship between the furfural yield and the partition coefficient can be observed under these experimental conditions, achieving the highest R value (4.4) in the presence of CaCl_2 , which provides the highest furfural yield (71%). In addition, the partition coefficient is lower for MgCl_2 ($R = 2.8$), although higher than in the case of using Al_2O_3 . It should also be noted that both furfural yield and the partition coefficient are lower when a mixture of $\gamma\text{-Al}_2\text{O}_3$ and CaCl_2 was used, which might be due to alumina favoring side reactions, as previously commented.

Takin into account that $\gamma\text{-Al}_2\text{O}_3$ favors secondary reactions, the influence of the reaction time has also been performed by using $\gamma\text{-Al}_2\text{O}_3$ without and with CaCl_2 in the reaction medium, and compared with the non-catalyzed process (in the absence of catalyst), without and with salt (Fig. 5). In all cases, higher conversion and furfural yield values were attained at 175°C in the presence of $\gamma\text{-Al}_2\text{O}_3$ and/or calcium chloride with respect to the non-catalyzed process. The use of this acid catalyst in the presence of CaCl_2 exhibited a much higher catalytic activity, even at short reaction times, attaining a xylose conversion and furfural yield of 97% and 55%, respectively, after 50 min of reaction (Fig. 5A). It can be observed that the furfural yield was lower than expected, achieving better results using only calcium chloride without a solid acid catalyst, with a conversion of xylose of 96% and a furfural yield of 71%, after 50 min at 175°C . This fact would demonstrate that $\gamma\text{-Al}_2\text{O}_3$ promoted the side reactions of furfural at high temperature, consequently decreasing the furfural yield (Fig. 5B) [28]. However, it should be noted that both xylose conversion and furfural yield after 15 min of reaction are higher by using a mixture of Al_2O_3 and CaCl_2 (66% and 44%, respectively) than those obtained by employing only CaCl_2 , thus confirming that the furfural yield decreases along the reaction due to the side reactions. Thus, in order to minimize secondary reactions and enhancing the furfural selectivity, the rest of the catalytic study will be performed at a lower reaction temperature and shorter reaction time (150°C and 30 min).

Firstly, the concentration of calcium chloride has been optimized in the absence of $\gamma\text{-Al}_2\text{O}_3$ (Fig. 6). According to the results previously obtained in glucose dehydration to HMF [42], the higher CaCl_2 concentration is employed, the higher value of both xylose conversion and furfural yield are achieved, achieving the maximum values in the

presence of 0.65 g CaCl₂ per g aqueous solution (48% and 21%, respectively), after 30 min at 150 °C. However, the catalytic activity does not improve when the amount of calcium chloride is near to the saturation value (0.85 g_{CaCl₂}·g_{aq.sol.}⁻¹). Therefore, the presence of CaCl₂ enhances the catalytic performance, being the optimal amount equal to 0.65 g_{CaCl₂}·g_{aq.sol.}⁻¹.

Next, the influence of the catalyst concentration has also been evaluated by varying the xylose:catalyst weight ratio (10:1-1:1) (Fig. 7), by using the previously optimized amount of 0.65 g_{CaCl₂}·g_{aq.sol.}⁻¹ and increasing the amount of catalyst, maintaining constant the concentration of xylose (0.15 g xylose in 1.5 mL water). It can be observed that xylose conversion is higher than 80% when alumina was incorporated, attaining similar values (90-94%) for xylose:catalyst weight ratios between 6:1 and 1:1. With respect to the furfural yield, a decrease was found when the amount of catalyst raised, which would corroborate that γ -Al₂O₃ enhances xylose conversion but favoring side reactions, consequently decreasing the furfural yield. Thus, maximum furfural yields (42-44%) were attained for xylose:catalyst weight ratio equal to 3:1 and 6:1. In the case of a xylose:catalyst weight ratio of 1:1, the furfural yield achieved was 33% in spite of xylose conversion also was high. Therefore, the optimum amount of catalyst should be that corresponding to a weight ratio of xylose:catalyst between 3:1 and 6:1, because a higher loading of alumina could favor secondary reactions, thus decreasing furfural yield.

Therefore, the kinetics of the dehydration process was studied at 150 °C, with γ -Al₂O₃ (xylose:catalyst weight ratio of 3:1) and 0.65 g_{CaCl₂}·g_{aq.sol.}⁻¹ (Fig. 8). It should be noted that unlike the results found at higher temperature (175 °C), both xylose conversion and furfural yield are considerably greater in presence of γ -Al₂O₃ and CaCl₂

with respect to values obtained only with CaCl_2 . It should be mentioned that xylose conversion and furfural yield values were 94% and 44% respectively after only 30 minutes of reaction, (Fig. 8), attaining almost full xylose conversion and a furfural yield of 55% after 50 min at the same temperature. In order to rule out the homogeneous contribution of soluble aluminum species, the analysis of Al in the reaction medium, after 50 min of reaction at 150 °C in the presence of CaCl_2 , has been carried out by ICP-MS. Thus, only 1.5 wt% of the total Al initially present in the catalyst was detected in the aqueous phase, so the contribution of soluble aluminum species was negligible in the dehydration of xylose to furfural. These results indicate that CaCl_2 improves the catalytic behavior of $\gamma\text{-Al}_2\text{O}_3$ at lower temperatures, and there may be a synergistic effect between both, minimizing side reactions, which would demonstrate that this salt can play a key role. Indeed, unlike the effect observed at 175 °C, the partition coefficient after 30 min at 150 °C was higher by using $\gamma\text{-Al}_2\text{O}_3$ and CaCl_2 together ($R=2.4$) than if only CaCl_2 was employed ($R=1.7$). Thus, the combined use of alumina and CaCl_2 at 150 °C improved the catalytic performance, enhancing furfural production which was quickly extracted by toluene and consequently increasing the partition coefficient. Considering that calcium cations could interact with the strongest acid sites of alumina and consequently decrease the side reactions that lead to furfural yield losses, $\gamma\text{-Al}_2\text{O}_3$ was put in contact with CaCl_2 under the same reaction conditions ($0.65 \text{ g}_{\text{CaCl}_2} \cdot \text{g}_{\text{aq.sol}}^{-1}$, 150 °C and 50 min) without xylose in the medium. This catalyst, denoted as $\text{exCa-Al}_2\text{O}_3$, was recovered and characterized by XPS in such a way that very low atomic concentration of Ca (0.35 at%) was detected on the catalyst surface. The catalytic behavior of $\text{exCa-Al}_2\text{O}_3$ has been also evaluated after 50 min at 150 °C without adding more CaCl_2 (Figure 8). It can be observed that this catalyst led to lower values of

xylose conversion and furfural yield (29 and 11%, respectively) than those found in presence of CaCl_2 and/or $\gamma\text{-Al}_2\text{O}_3$. Thus, the improvement of catalytic behavior is not favored by this cation exchange. Therefore, it was necessary a more exhaustive analysis to prove the existence of this synergistic effect between CaCl_2 and catalyst.

In this sense, García-Sancho *et al.* [42] have previously found that calcium cations can alter the anomeric equilibrium of D-glucose, enhancing its dehydration rate to HMF since Ca^{2+} favored the formation of the α -D-glucopyranose anomer. It was observed that the combination of CaCl_2 and an acid catalyst, $\gamma\text{-Al}_2\text{O}_3$, provided high HMF yields at very short reaction times. These results coincided with those found by Rasrendra *et al.* [34], who reported that anions had a less effect for glucose conversion than cations. As it has been mentioned, alkaline earth cations can form bidentate complexes with different carbohydrates [53, 54]. The stability of the sugar-cation complex depends on both the stereochemical disposition of the hydroxyl groups of sugar and the Lewis acid strength of the cation [55-59]. The most favorable configuration of a carbohydrate to interact with a divalent cation is the ax.-eq.-ax. (positions of OH groups at C1, C2 and C3 in pyranose form, respectively; ax: axial and eq: equatorial positions) configuration, but other cyclic sugars without this sequence, like D-glucose, can form weaker Ca^{2+} complexes by interaction of alkaline earth metal cations with two oxygen atoms [42, 53, 54]. In the case of xylose, the presence of Ca^{2+} could influence on the anomeric distribution of xylose, which could follow a similar trend as that found in the case of glucose. As mentioned, sugar complexes with alkaline earth halides are weak and unstable in water, due to the competition of water and sugar for the cation. The interaction of cations with the oxygen atom of hydroxyl groups is regarded as the main driving force for complex formation [59]. Therefore, it would be

possible that CaCl_2 accelerates xylose dehydration as was found in the case of glucose through complexation with salts. It was previously demonstrated that the addition of CaCl_2 induced the displacement of the β -form of D-glucose towards the α -conformer, as previously commented [39]. On the other hand, Enslow *et al.* [36] concluded that the presence of alkaline salts increased the α -xylopyranose/ β -xylopyranose ratio, although it has been reported that the interaction between carbohydrates and divalent cations is much stronger than those with monovalent cations [39, 40].

In order to verify these assumptions, $^1\text{H-NMR}$ spectroscopy at room temperature has been determined for different solutions of D-xylose in presence of $\gamma\text{-Al}_2\text{O}_3$ and alkaline earth metal chlorides in deuterated water (Fig. 10). The $^1\text{H-NMR}$ spectrum of D-xylose in D_2O (Fig. 9A) shows the equilibrium of both conformers, α and β (Scheme 1), although the intensity of α -xylopyranose is much higher. This same trend was detected after incorporation of $\gamma\text{-Al}_2\text{O}_3$, CaCl_2 or MgCl_2 to the xylose solution (Fig. 9B, C and D, respectively). It has also been reported that the furanose content at equilibrium in water is usually less than 1%, at 30 °C [60]. Thus, the α -xylopyranose/ β -xylopyranose ratio is higher than 1 in all cases, which indicates that the α -xylopyranose is favored at room temperature in spite of the addition of alumina or alkaline earth salts. This fact may be due to the interaction between xylose and cations is weaker than that found for other carbohydrates containing ax.-eq.-ax. configurations, such as ribose and galactose, since the hydroxyl groups in β -xylopyranose are in eq.-eq.-eq. orientation and those in α -xylopyranose are in ax.-eq.-eq. orientation.

On the other hand, Mikkola *et al.* reported that the ratio of α -xylopyranose/ β -xylopyranose in aqueous solution increases with the temperature [60]. In order to check

this fact, the solutions previously measured at room temperature were heated in a sealed NMR tube at 110 °C for 24 h, and the corresponding spectra were registered (Fig. 10). In our case, differently to that observed by Mikkola *et al.*, the β form is favored with respect to the α form in all cases, although the analysis conditions were not similar to those used by Mikkola *et al.*, since they obtained the $^1\text{H-NMR}$ spectra after 1 h at each temperature, between 20-100 °C. However, the trend of α -xylopyranose/ β -xylopyranose ratio after heating is not the same in all cases, being considerably higher in the case of xylose dissolved in D_2O with CaCl_2 (Fig. 10C). Thus, the presence of CaCl_2 at high temperature promotes the formation of the α anomer in comparison with the α -xylopyranose/ β -xylopyranose ratio obtained with $\gamma\text{-Al}_2\text{O}_3$, MgCl_2 or in absence of catalyst or salt (0.94 versus 0.53-0.57) (Figs. 10A, 10B and 10D). It should be also noted that the peaks corresponding to the signal of the furan ring began to appear in the case of xylose with $\gamma\text{-Al}_2\text{O}_3$ (Fig. 10B).

In a previous mechanistic study, Nimlos *et al.* concluded that the intramolecular rearrangement is more favorable for furfural formation than the pyranose ring opening [61]. They also affirmed that the dehydration reaction is favored at the C2OH position of xylopyranose with respect to C1OH and the fragmentation products increased when dehydration started at C3OH or C4OH. Later, Enslow *et al.* reported that dehydration of β -xylopyranose at the C2 position was energetically more favorable than at the C1 position, but both C1OH and C2OH initiated dehydration was possible in the case of α -xylopyranose due to the hydroxyl group in the axial position of the α conformer was more easily protonated and removed as water than the equatorial one [36]. These authors also observed that the initial dehydration at C1OH group occurred more quickly than that initiated at C2OH group when alkaline halides were added to the reaction

medium. Taking into account these conclusions and the results obtained by $^1\text{H-NMR}$ spectroscopy, it would be possible that dehydration of xylose is considerably enhanced in presence of CaCl_2 because of this salt increases the α -xylopyranose/ β -xylopyranose ratio, in such a way that xylose dehydration could take place through both C1OH and C2OH pathways, being faster in the first case. Thus, a similar effect to that found by Enslow *et al.* [36] for alkaline halides would explain the improved xylose conversion and furfural yield observed with CaCl_2 . However, this improvement was not detected in the presence of MgCl_2 , since this salt did not rise the α -xylopyranose/ β -xylopyranose ratio, as inferred from its $^1\text{H-NMR}$ spectrum (Fig. 10D), which would explain its worse catalytic performance. Therefore, this fact could justify the improvement of catalytic performance found in presence of CaCl_2 at 175 °C with respect to the rest of cases. Once that first dehydration was carried out, the high reaction temperature, 175 °C, favors the next dehydration steps, and consequently the furfural production, increasing the partition coefficient since the existence of side reactions is decreased due to the absence of acid sites.

However, different results in the dehydration process were attained at lower temperature (150 °C) and the best catalytic performance was found for a cooperative contribution of both CaCl_2 and $\gamma\text{-Al}_2\text{O}_3$. Considering that $^1\text{H-NMR}$ spectroscopy has demonstrated that CaCl_2 increases the α -xylopyranose/ β -xylopyranose ratio and the presence of furfural is only detected in the spectrum of $\gamma\text{-Al}_2\text{O}_3$, this synergistic effect between salt and Lewis acid catalyst could be explained in such a way that CaCl_2 provides the correct anomer for efficient dehydration and $\gamma\text{-Al}_2\text{O}_3$ accelerates and promotes the transformation of D-xylose to furfural when the reaction is carried out at

150 °C, since the losses of furfural due to the unwanted side reactions are minimized under these reaction conditions.

On the other hand, the reuse of γ -Al₂O₃ has also been evaluated in the presence of 0.65 g_{CaCl₂}·g_{aq.sol.}⁻¹ with a xylose:catalyst weight ratio of 3:1 at 150 °C for 50 min, without any type of treatment after each catalytic cycle (Fig. 11). The catalyst remained inside the reactor, without any type of treatment, and after each catalytic run a new mixture (xylose, CaCl₂, water and toluene) was added to carry out the reaction under identical experimental conditions. It can be observed that the catalyst maintains its activity after ten catalytic runs in such a way that the conversion values only decrease from 98% to 89%, after the tenth catalytic cycle, maintaining the furfural yield between 47%-66% throughout the cycles. However, it should be noted that a small increase for furfural yield can be found between different catalytic runs, mainly between 1st-2nd and 7th-8th cycles. This fact is probably due to a fraction of furfural formed could be retained on the catalytic surface after the first cycle, which could be desorbed after heating the new reaction mixture in the next catalytic run, enhancing the furfural yield for this second cycle. In order to corroborate this fact, the first reaction cycle was carried out again, but the used γ -Al₂O₃ catalyst was washed firstly with toluene and then with water, under vacuum filtration, to facilitate the desorption of furfural adsorbed on the catalyst surface. The analysis of these solvents after washing by HPLC has allowed to detect the presence of furfural in both phases. However, the absence of xylose in the aqueous phase would indicate that this compound is not adsorbed on the surface of γ -Al₂O₃, or the washing is not enough for its desorption because its interaction is stronger. Therefore, we could conclude that these variations in furfural yields throughout the cycles during the reuse of the catalyst, are due to the retention of the furfural formed on

the surface of $\gamma\text{-Al}_2\text{O}_3$. This fact has been corroborated by CHN analysis of spent catalyst which showed a carbon content of 5.98 wt% higher than 0.05 wt% detected for fresh alumina. Likewise, the catalyst has been recovered after 1st catalytic run without washing ($\gamma\text{-Al}_2\text{O}_3$ (u)) and after washing with toluene and water ($\gamma\text{-Al}_2\text{O}_3$ (w)) for their characterization. Thus, it can be checked that both BET surface area and pore volume considerably decrease for $\gamma\text{-Al}_2\text{O}_3$ (u) (Table 1). Moreover, the average pore diameter slightly increases which confirms that the smallest pores are blocked by adsorbed species. However, this fact is much less abrupt in the case of $\gamma\text{-Al}_2\text{O}_3$ (w) which corroborates again that the washing with toluene and water allows to extract an important fraction of adsorbed species, furfural among them, as detected in the analysis of washing solvents. It has also been demonstrated by XRD that the catalyst preserves its structure after reaction (not shown), since typical diffraction lines associated to gamma-aluminum oxide remain after the catalytic process (PDF 00-029-1486)

Finally, the use of $\gamma\text{-Al}_2\text{O}_3$ and CaCl_2 has been evaluated to obtain furfural from liquors obtained from olive stones, at 175 °C after 50 min (Fig. 12). This catalytic test has been realized at higher temperature in order to facilitate hydrolysis reaction, since the hemicellulose hydrolysis carried out in the previous treatment was not complete. It can be checked that the synergistic affect between $\gamma\text{-Al}_2\text{O}_3$ and CaCl_2 has allowed to increase the furfural yield from 53% for the non-catalyzed process until 85%. Therefore, the combination of $\gamma\text{-Al}_2\text{O}_3$ and CaCl_2 can be also employed for furfural production from lignocellulosic biomass.

4. Conclusions

$\gamma\text{-Al}_2\text{O}_3$ has demonstrated to be an active catalyst for the dehydration of xylose to furfural, since it possesses weak and strong Lewis acid sites, as inferred from the

NH₃-TDP and pyridine adsorption coupled to FTIR spectroscopy. The use of a water:toluene biphasic system has allowed to attain xylose conversion and furfural yield values of 86% and 26%, respectively, after 50 min at 175°C in presence of γ -Al₂O₃. The addition of different alkaline earth metal chlorides, such as CaCl₂ and MgCl₂, in order to decrease secondary reactions has been evaluated, in such a way that an increase in partition coefficient, which indicates the proportion of furfural between the organic and aqueous phases, was observed. In this sense, CaCl₂ was much more effective due to the presence of calcium affected to the α -xylopyranose/ β -xylopyranose anomeric equilibrium and favored the formation of the α anomer, as revealed the ¹H NMR spectra, which facilitated the dehydration process. A synergistic effect between γ -Al₂O₃ and CaCl₂ was found, attaining almost full xylose conversion and a furfural yield of 55% after 50 min at 150°C since CaCl₂ increased the α -xylopyranose/ β -xylopyranose ratio and γ -Al₂O₃ accelerated the furfural production in these reaction conditions in which the unwanted side reactions were minimized. The catalytic activity of γ -Al₂O₃ was also stable and, without any pretreatment, for ten catalytic cycles, with almost full xylose conversion and maintaining an average furfural yield of 57%. The synergistic effect between CaCl₂ and γ -Al₂O₃ was also found by using hemicellulosic liquors obtained from olive stones as source of carbohydrates, achieving until a furfural yield of 83% after 50 min at 175°C, in comparison with the use of the individual components.

Acknowledgements

The authors want express their gratitude to the Spanish Ministry of Economy and Competitiveness (CTQ2015-64226-C03-3-R project) and FEDER (European Union) funds about financial support. J.A.C. and C.G.-S. thank to the Malaga

University for the financial support. L.S.C. gratefully acknowledges support from Spanish MINECO via the concession of a Ramon y Cajal contract (RYC-2015-17109).

References

- [1] In T. Werpy and G. Peterson (Editors), *Top Value Added Chemicals from Biomass*, Vol. Volumen 1, Pacific Northwestern National Laboratory; 2004.
- [2] M. Stocker, *Angew. Chem.-Int. Edit.*, 47 (2008), pp. 9200-9211.
- [3] R. van Putten, J. van der Waal, E. de Jong, C. Rasrendra, H. Heeres, J. de Vries, *Chem. Rev.*, 113 (2013), pp. 1499-1597.
- [4] D. Alonso, J. Bond, J. Dumesic, *Green Chem.*, 12 (2010), pp. 1493-1513.
- [5] T. Wang, M. Nolte, B. Shanks, *Green Chem.*, 16 (2014), pp. 548-572.
- [6] G. Garrote, E. Falqué, H. Domínguez, J.C. Parajó, *Bioresource Technol.*, 98 (2007), pp. 1951-1957.
- [7] W.G. Glasser, R.K. Jain, M.A. Sjöstedt, *Thermoplastic pentosan-rich polysaccharides from biomass*, Vol. US Patent 5430142, US Patent; 1995.
- [8] R. Mariscal, P. Maireles-Torres, M. Ojeda, I. Sádaba, M. López Granados, *Energ. Environ. Sci.*, 9 (2016), pp. 1144-1189.
- [9] M.J. Antal, T. Leesomboon, W.S. Mok, *Carbohyd. Res.*, 217 (1991), pp. 71-85.
- [10] R. Karinen, K. Vilonen, M. Niemelä, *ChemSusChem*, 4 (2011), pp. 1002-1016.
- [11] In K.J. Zeitsch (Editors), *The chemistry and technology of furfural and its many by-products*, Elsevier Science; 2000.
- [12] R. Weingarten, G. Tompsett, W. Conner, G. Huber, *J. Catal.*, 279 (2011), pp. 174-182.
- [13] A. Mittal, S. K. Black, T. B. Vinzant, M. O'Brien, M. P. Tucker, D. K. Johnson, *ACS Sustain. Chem. Eng.*, 5 (2017), pp. 5694-5701.
- [14] J. N. Chheda, Y. Román-Leshkov, J. A. Dumesic, *Green Chem.*, 9 (2007), pp. 342-350.
- [15] E. I. Gürbüç, S. G. Wettstein, J. A. Dumesic, *ChemSusChem*, 5 (2012), pp. 383-387.
- [16] C.L. Burket, S. Sabesan, *Process for furfural production from biomass*, Vol. Volume US Patent 0157697A1, US Patent; 2012.
- [17] T.Y. Zhang, R. Kumar, C.E. Wyman, *RSC Adv.*, 3 (2013), pp. 9809-9819.
- [18] N. Shi, Q.Y. Liu, Q. Zhang, T.J. Wang, L.L. Ma, *Green. Chem.*, 15 (2013), pp. 1967-1974.
- [19] Y. Yang, C. W. Hu, M. M. Abu-Omar, *ChemSusChem*, 5 (2012), pp. 405-410.
- [20] A. Dias, M. Pillinger, A. Valente, *J. Catal.*, 229 (2005), pp. 414-423.
- [21] R. Weingarten, G. Tompsett, W. Conner, G. Huber, *J. Catal.*, 279 (2011), pp. 174-182.
- [22] I. Agirrezabal-Telleria, A. Larreategui, J. Requies, M. Guemez, P. Arias, *Bioresource Technol.*, 102 (2011), pp. 7478-7485.
- [23] A. Dias, M. Pillinger, A. Valente, *Micropor. Mesopor. Mat.*, 94 (2006), pp. 214-225.
- [24] X. Shi, Y. Wu, H. Yi, G. Rui, P. Li, M. Yang, G. Wang, *Energies*, 4 (2011), pp. 669-684.

- [25] P. Zhou, Z. Zhang, *Catal. Sci. Technol.*, 6 (2016), pp. 3694-3712.
- [26] J. He, H. Li, S. Saravanamurugan, S. Yang, *ChemSusChem*, 12 (2019), pp. 347-378.
- [27] J.E. Romo, N.V. Bollar, C.J. Zimmermann, S.G. Wettstein, *ChemCatChem*, 10 (2018), pp. 4819-4830.
- [28] C. Garcia-Sancho, I. Agirrezabal-Telleria, M. Guemez, P. Maireles-Torres, *Appl. Catal. B-Environ.*, 152 (2014), pp. 1-10.
- [29] C. Song, H. Liu, Y. Li, S. Ge, H. Wang, W. Zhu, Y. Chang, C. Han, H. M. Li, *Chin. J. Chem.*, 32 (2014), pp. 434-442.
- [30] J. Kruger, V. Choudhary, V. Nikolakis, D. Vlachos, *ACS Catal.*, 3 (2013), pp. 1279-1291.
- [31] W. Zeng, D. Cheng, F. Chen, X. Zhan, *Catal. Lett.*, 133 (2009), pp. 221-226.
- [32] S. You, N. Park, E. Park, M. Park, *J. Ind. Eng. Chem.*, 21 (2015), pp. 350-355.
- [33] S. You, Y. Kim, E. Park, *Reac. Kinet. Mech. Catal.*, 111 (2014), pp. 521-534.
- [34] G. Marcotullio, W. De Jong, *Green Chem.*, 12 (2010), pp. 1739-1746.
- [35] G. Marcotullio, W. de Jong, *Carbohydr. Res.*, 346 (2011), pp. 1291-1293.
- [36] K.R. Enslow, A.T. Bell, *ChemCatChem*, 7 (2015), pp. 479-489.
- [37] C. Rasrendra, I. Makertihartha, S. Adisasmito, H. Heeres, *Top. Catal.*, 53 (2010), pp. 1241-1247.
- [38] Y. Roman-Leshkov, J. Dumesic, *Top. Catal.*, 52 (2009), pp. 297-303.
- [39] J. Teychené, H. Roux-De Balman, S. Galier, *Carbohydr. Res.*, 448 (2017), pp. 118-127.
- [40] P.K. Banipal, A.K.C.N. Hundal, T.S. Banipal, *Carbohydr. Res.*, 345 (2010), pp. 2262-2271.
- [41] E. Combs, B. Cinlar, Y. Pagan-Torres, J. Dumesic, B. Shanks, *Catal. Commun.*, 30 (2013), pp. 1-4.
- [42] C. García-Sancho, I. Fúnez-Núñez, R. Moreno-Tost, J. Santamaría-González, E. Pérez-Inestrosa, J.L.G. Fierro, P. Maireles-Torres, *Appl. Catal. B-Environ.*, 206 (2017), pp. 617-625.
- [43] D. Amendola, D.M. De Faveri, I. Egües, L. Serrano, J. Labidi, G. Spigno, *Bioresource Technol.*, 107 (2012), pp. 267-274.
- [44] M.J Campos Molina, M. López Granados, A. Gervasini, P. Carnit, *Catal. Today*, 254 (2015), pp. 90-98.
- [45] P. Berteau, B. Delmon, A. Crucq, A. Frennet, *Catal. Today*, 5 (1989), pp. 121-137.
- [46] J. Gallo, C. Bisio, G. Gatti, L. Marchese, H. Pastore, *Langmuir*, 26 (2010), pp. 5791-5800.
- [47] A. Ramirez, B. Lopez, L. J. Sierra, *Phys. Chem. B*, 107 (2003), pp. 9275-9280.
- [48] C. García-Sancho, J.A. Cecilia, A. Moreno-Ruiz, J.M. Mérida-Robles, J. Santamaría-González, R. Moreno-Tost, P. Maireles-Torres, *Appl. Catal. B-Environ.*, 179 (2015), pp. 139-149.
- [49] J. Chan, Y. Zhang, *ChemSusChem*, 2 (2009), pp. 731-734.
- [50] C. McNeff, D. Nowlan, L. McNeff, B. Yan, R. Fedie, *Appl. Catal. A-Gen.*, 384 (2010), pp. 65-69.
- [51] C. Rasrendra, J. Soetedjo, I. Makertihartha, S. Adisasmito, H. Heeres, *Top. Catal.*, 55 (2012), pp. 543-549.
- [52] X. Wu, J. Fu, X. Lu, *Bioresource Technol.*, 119 (2012), pp. 48-54.
- [53] S. Tyrlik, D. Szerszen, M. Olejnik, W. Danikewicz, *J. Mol. Catal. A-Chem.*, 106 (1996), pp. 223-233.

- [54] C. Yang, X. Lu, W. Lin, X. Yang, J. Yao, Chem. Res. Chin., U22 (2006), pp. 524-532
- [55] J. Angyal, Adv. Carbohyd. Chem. Biochem., 49 (1991), p. 19-35.
- [56] J. Angyal, Adv. Carbohyd. Chem. Biochem., 47 (1989), p. 1-43.
- [57] J. Angyal, Adv. Carbohyd. Chem. Biochem., 42 (1984), p. 15-68.
- [58] K. Bock, C. Pedersen, Adv. Carbohyd. Chem. Biochem., 41 (1983), p. 27-66.
- [59] A. Rendleman, Adv. Carbohyd. Chem., 21 (1966), p. 209-271.
- [60] J.P. Mikkola, R. Sjoholm, T. Salmi, P. Maki-Arvela, Catal. Today, 48 (1999), pp. 73-81.
- [61] M.R. Nimlos, X. Qian, M. Davis, M. E. Himmel, D. K. Johnson, J. Phys. Chem. A, 110 (2006), pp. 11824-11838.

Journal Pre-proof

List of captions

Figure 1. Nitrogen adsorption (solid symbols)-desorption (open symbols) isotherms (A) and pore size distribution curve (B) of the γ -Al₂O₃ catalyst.

Figure 2. NH₃-TPD curve of the γ -Al₂O₃ catalyst.

Figure 3. FTIR spectra of adsorbed pyridine over γ -Al₂O₃ outgassed at different temperatures.

Figure 4. (A) Influence of adding CaCl₂ (0.65 g·g_{aq.sol.}⁻¹), MgCl₂ (0.39 g·g_{aq.sol.}⁻¹) and/or γ -Al₂O₃ on xylose conversion and furfural yield at 175 °C after 50 min (xylose:catalyst weight ratio= 3:1). (B) Furfural yield as function of the partition coefficient of furfural in both phases (175 °C, 50 min).

Figure 5. Xylose conversion (A) and furfural yield (B) as a function of reaction time in presence of γ -Al₂O₃ and/or CaCl₂ (175 °C, 0.65 g_{CaCl₂} ·g_{aq.sol.}⁻¹, 0.05 g of γ -Al₂O₃ and xylose:catalyst weight ratio = 3:1).

Figure 6. Effect of CaCl₂ concentration on xylose conversion and furfural yield without catalyst at 150 °C after 30 min.

Figure 7. Xylose conversion and furfural yield as function of xylose:catalyst weight ratio for γ -Al₂O₃ at 150 °C and 30 min in presence of 0.65 g_{CaCl₂} ·g_{aq.sol.}⁻¹ (0.15, 0.05, 0.025 and 0.015 g of γ -Al₂O₃ for xylose:catalyst weight ratio = 1:1, 3:1, 6:1 and 10:1, respectively).

Figure 8. Evolution of xylose conversion (solid symbols) and furfural yield (open symbols) with the reaction time in presence of γ -Al₂O₃ and/or CaCl₂ and exCa-Al₂O₃ (150 °C, 0.65 g_{CaCl₂} ·g_{aq.sol.}⁻¹, 0.05 g of γ -Al₂O₃ and xylose:catalyst weight ratio = 3:1).

Figure 9. ¹H NMR spectra of xylose in D₂O (A), before and after addition of Al₂O₃ (B), CaCl₂ (C) and MgCl₂ (D) at room temperature.

Figure 10. ¹H NMR spectra of xylose in D₂O (A), with Al₂O₃ (B), CaCl₂ (C) and MgCl₂ (D) after 24 h at 110 °C.

Figure 11. Reutilization study for the γ -Al₂O₃ catalyst at 150°C after 50 min in the presence of 0.65 g_{CaCl₂}·g_{aq.sol.}⁻¹ (0.05 g of γ -Al₂O₃ and xylose/catalyst weight ratio of 3:1).

Figure 12. Influence of adding Al₂O₃ and/or CaCl₂ (0.65 g·g_{aq.sol.}⁻¹) on furfural yield for xylose solutions from olive stones at 175 °C after 50 min (0.05 g of γ -Al₂O₃ and xylose:catalyst weight ratio= 3:1).

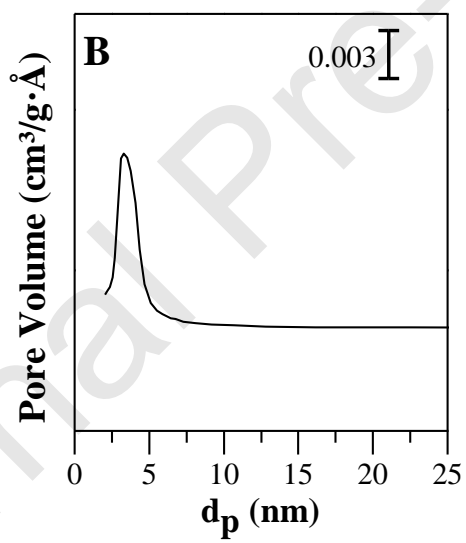
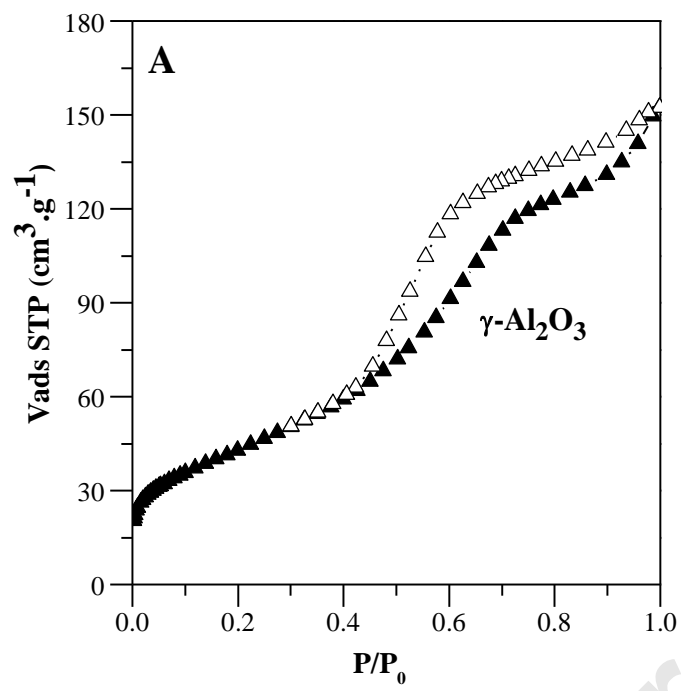


Figure 1

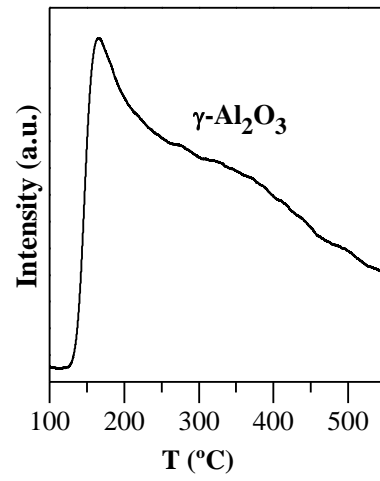


Figure 2

Journal Pre-proof

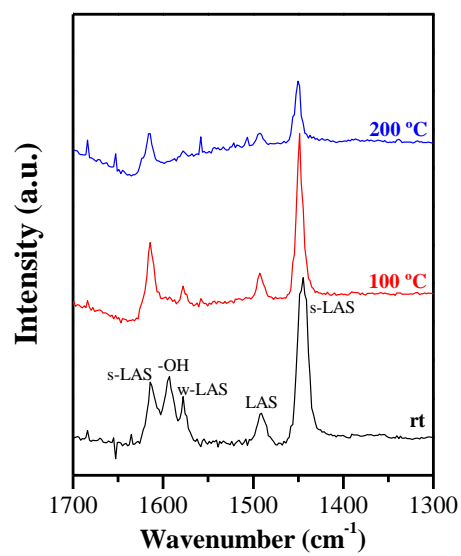


Figure 3

Journal Pre-proof

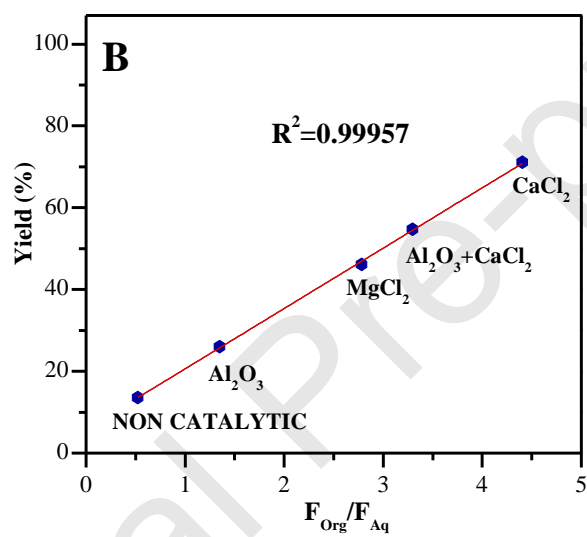
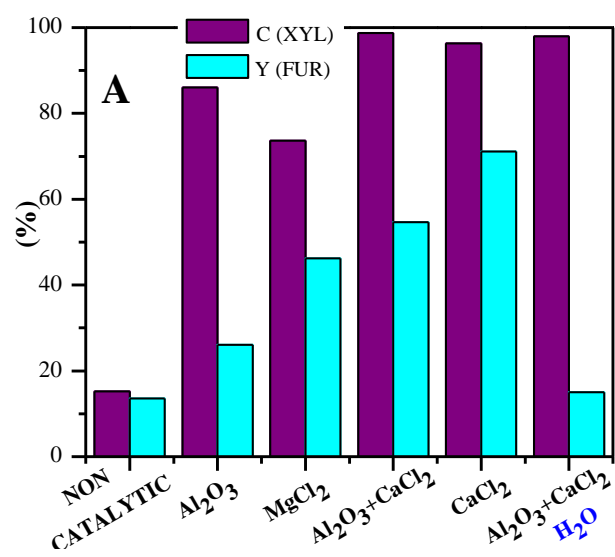


Figure 4

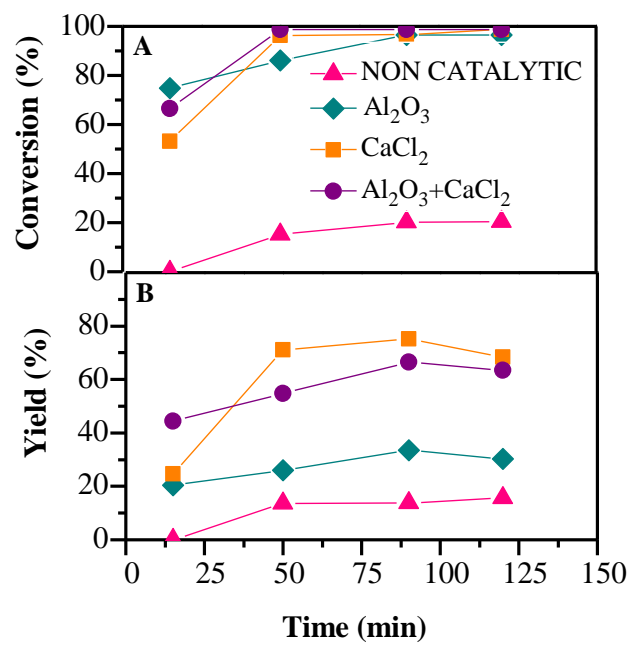


Figure 5

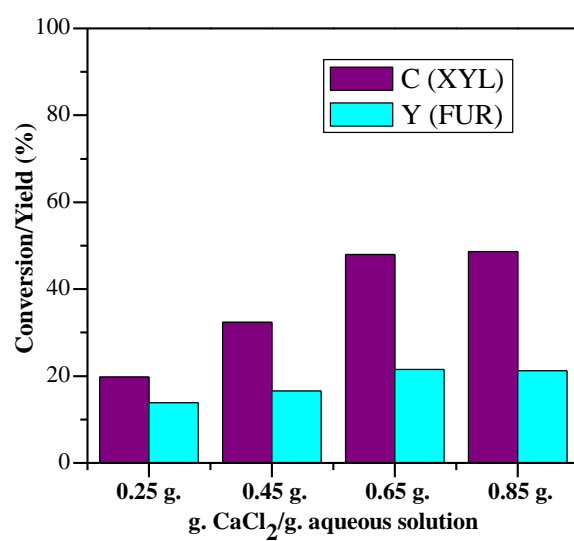


Figure 6

Journal Pre-proof

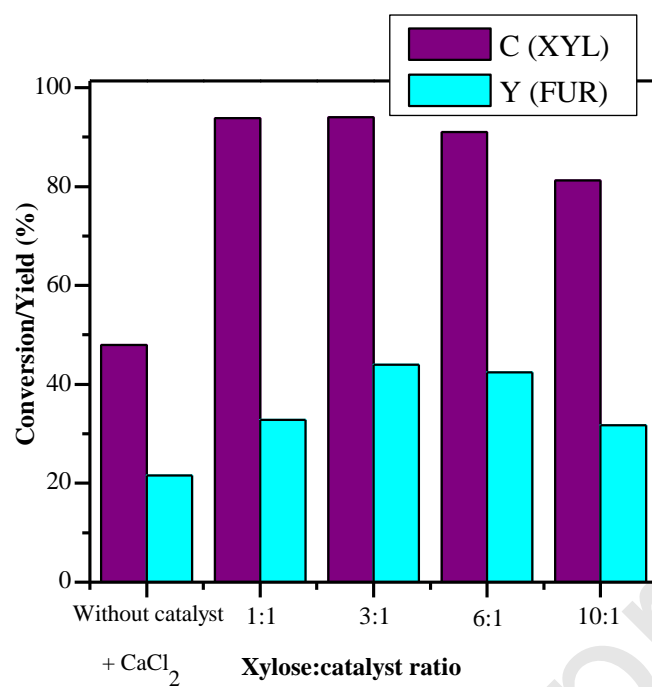


Figure 7

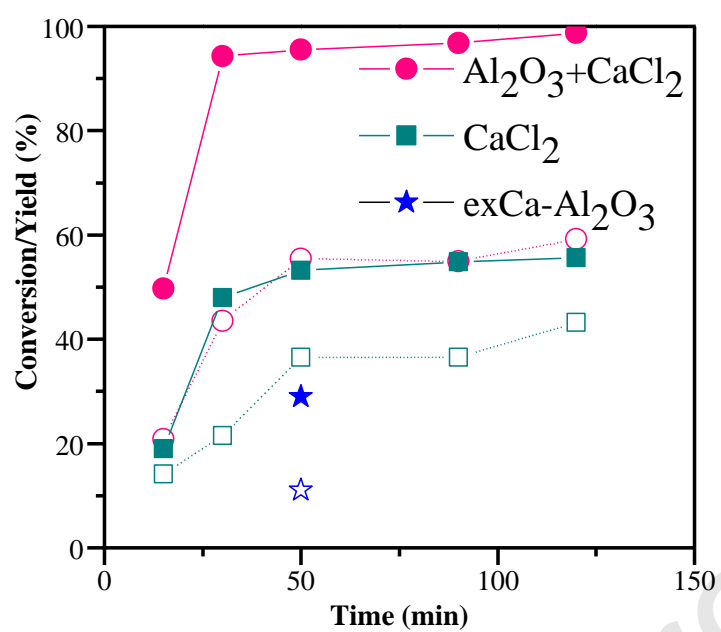


Figure 8

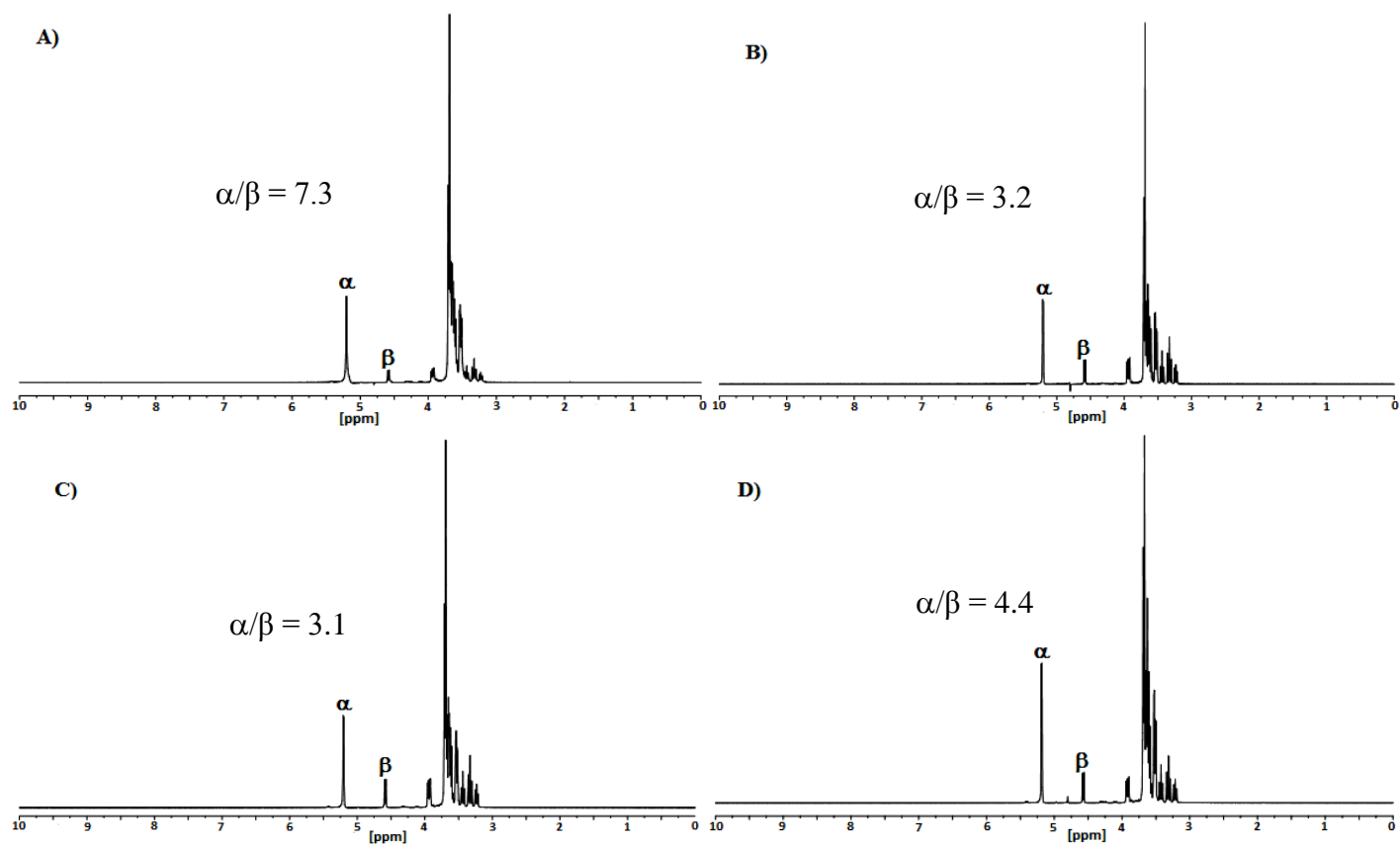


Figure 9

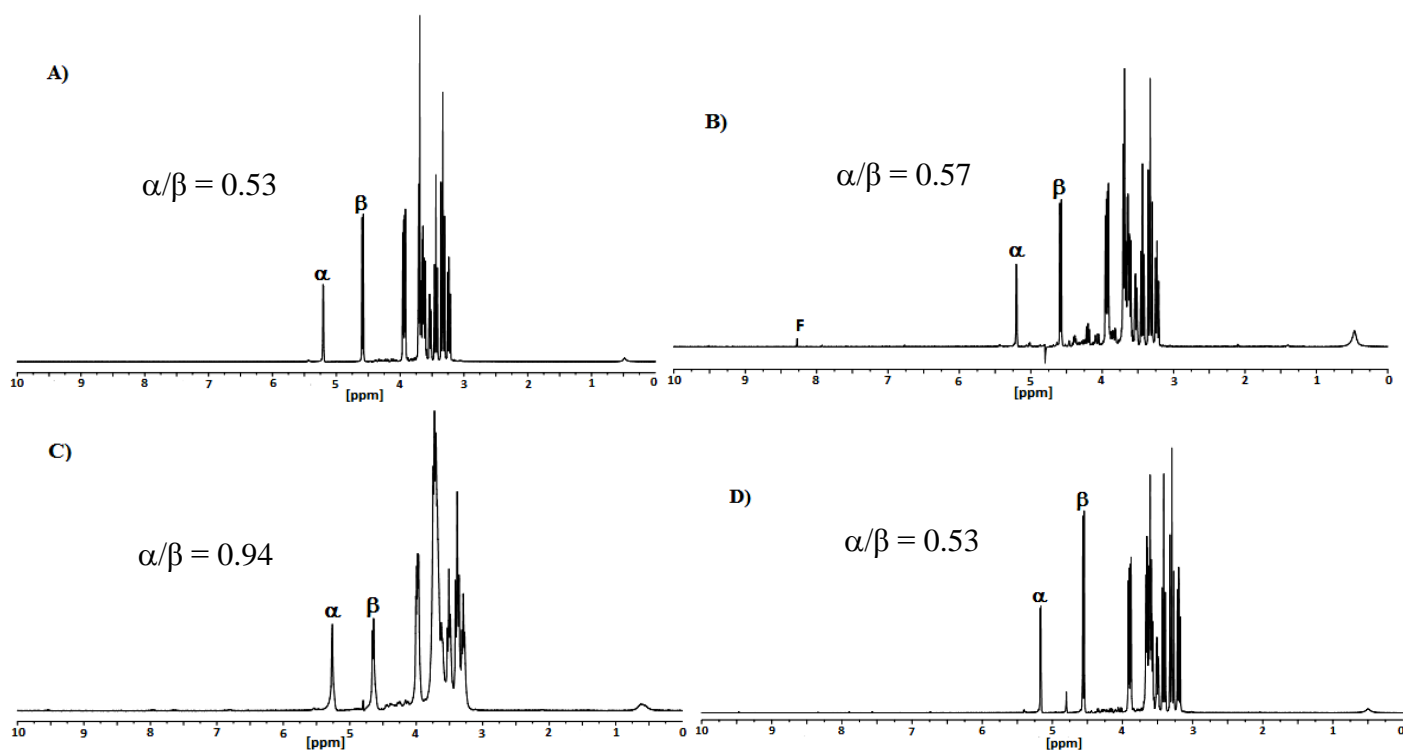


Figure 10

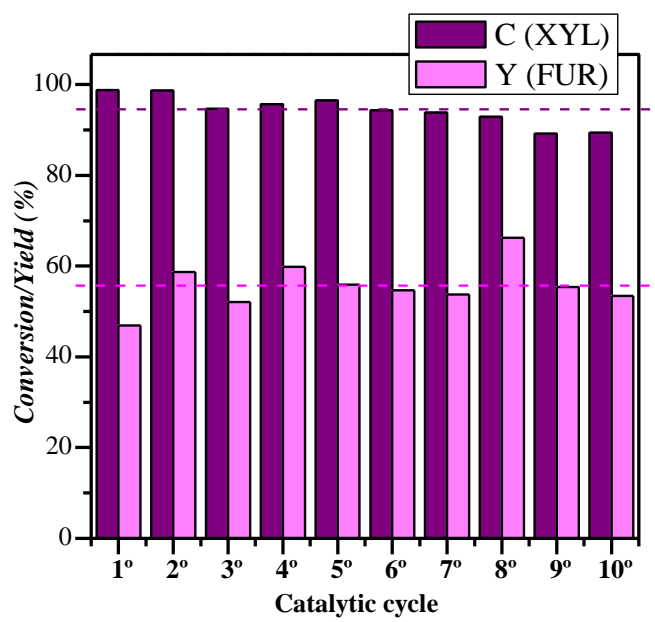


Figure 11

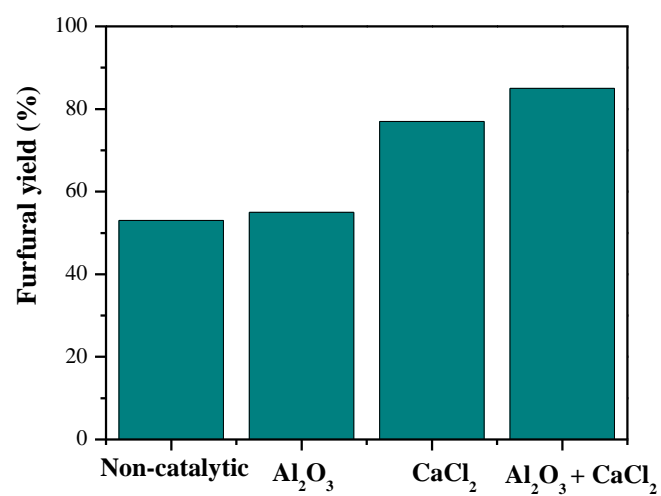
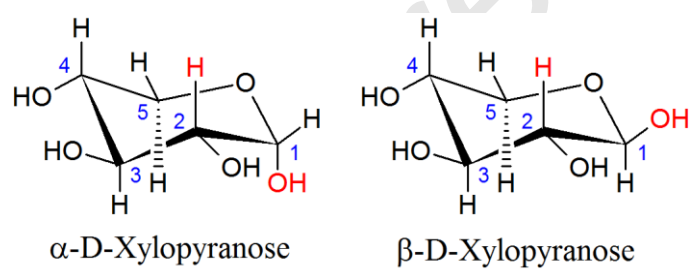


Figure 12



Scheme 1. Isomers of xylose.

Table 1. Textural and acidic properties of catalysts.

Sample	S_{BET} ($\text{m}^2 \cdot \text{g}^{-1}$)	V_{P} ($\text{cm}^3 \cdot \text{g}^{-1}$)	Pore size (nm)	$\mu\text{moles NH}_3 \cdot \text{g}_{\text{cat}}^{-1}$
$\gamma\text{-Al}_2\text{O}_3$	158	0.236	4.7	478
$\gamma\text{-Al}_2\text{O}_3$ (u)	36	0.056	5.7	—
$\gamma\text{-Al}_2\text{O}_3$ (w)	123	0.140	5.3	—

Journal Pre-proof